J|A|C|S COMMUNICATIONS

Published on Web 11/20/2009

Spectroscopic STM Studies of Single Gold(III) Porphyrin Molecules

Stefan Müllegger,*,† Wolfgang Schöfberger,*,‡ Mohammad Rashidi,† Lorenz M. Reith,‡ and Reinhold Koch†

Department of Solid State Physics and Institute of Inorganic Chemistry, Center for Nanobionics and Photochemical Sciences (CNPS), Johannes Kepler University, Altenbergerstrasse 69, 4040 Linz, Austria

Received October 1, 2009; E-mail: stefan.muellegger@jku.at; wolfgang.schoefberger@jku.at

Low-temperature scanning tunneling microscopy (LT-STM), a well-established technique for single-molecule investigations in an ultrahigh vacuum (UHV) environment,[1,2] has been used here to study the electronic properties of Au(III) 5,10,15,20-tetraphenylporphyrin (AuTPP) molecules on a gold surface. In particular, we present real-space images and local scanning tunneling spectroscopy (STS) data of the frontier molecular orbitals (MOs) of AuTPP and compare them with density functional theory (DFT) results.

Gold(III) porphyrins are among the most powerful electron acceptors in the series of tetrapyrrole-based photosensitizers.[3] They are considered as potential chemotherapeutics[4] and have been successfully employed as photonucleases for double-strand cleavage of DNA.[5] To date, the optical and electrochemical properties have been investigated only on ensembles of various Au(III) porphyrins in solution.[6,7] Ou et al.[8] reported on the influence of meso substituents on the macrocycle, which affect the specific location of the electrochemical reduction process within the molecule.

For the single-molecule investigations presented here, we chose a single-crystal surface of the chemically inert noble metal gold as substrate. The Au(111) surface is well-known for its $22 \times \sqrt{3}$ "herringbone" superstructure (Figure 1) that offers a regularly nano-patterned array of "kink" sites[9] at which molecules selectively adsorb[10] (Figure 1, right inset). AuTPP was chemically synthesized and thermally evaporated out of a glass tube onto Au(111) under UHV conditions (base pressure $<5 \times 10^{-11}$ mbar).

Figure 2a−d shows high-resolution constant-current STM images of a single AuTPP molecule taken at different bias voltages. Increased signal intensity is observed atop different structural elements of the molecule. In particular, the pyrroles of the macrocycle and the phenyl substituents can be clearly discerned. As a visual guide, the chemical structure is indicated in Figure 2c. Within a voltage range of −1.3 to +0.2 V, the appearance of AuTPP is almost bias-independent (Figure 2a,c,d). Characteristic protrusions are observed at the positions of the pyrroles and weaker ones on the phenyl substituents. Although AuTPP in the gas phase is fourfold-symmetric, the STM images of the adsorbed molecules show a reduced twofold symmetry.[11] Recent studies of porphyrins on Au(111), Ag(111), and Cu(111) revealed an alternating out-of-plane bending of the pyrroles in the macrocycle by ∼20°, leading to a so-called saddle conformation. Moreover, the phenyl substituents were found to be rotated with a dihedral angle (Φ) of 35−65° with respect to the macrocycle.[11−14] In accordance with those studies, we attribute the symmetry reduction of AuTPP to an analogous saddle-shaped distortion. At +0.9 V, on the other hand, the STM image of AuTPP changes significantly (Figure 2b). Four bright protrusions centered over the meso carbon atoms of the macrocycle become dominant, whereas the contributions of the pyrroles are suppressed. The bias dependence in STM originates from tunneling into different unoccupied MOs or out of different occupied MOs once they become energetically aligned with the tip Fermi level at a certain bias voltage.

† Department of Solid State Physics.
‡ Center for Nanobionics and Photochemical Sciences.

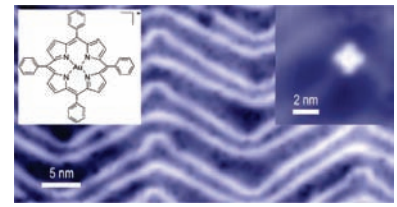

Figure 1. STM image of the Au(111) surface, which exhibits a herringbone superstructure. Insets: (left) chemical structure of AuTPP; (right) STM image of a single AuTPP molecule adsorbed at a "kink" site on Au(111).

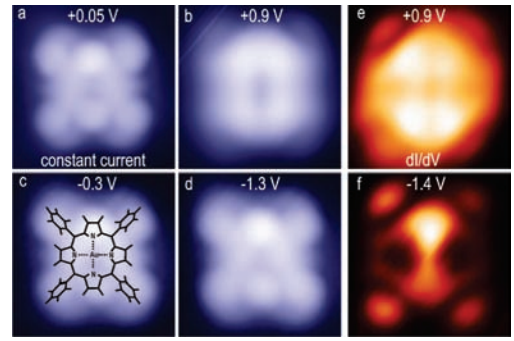

Figure 2. (a−d) High-resolution constant-current STM images (20 pA) recorded at 7 K and different bias voltages, as indicated in the figures. (e−f) Experimental d*I*/d*V* maps of AuTPP taken under constant-current conditions.

Figure 3a shows a tunneling spectrum obtained by ramping the bias voltage from −2 to +1.3 V while keeping the tip at a constant height over the center of AuTPP. Enhanced tunneling conductivity is clearly observed at certain bias voltages. The steplike shoulder around −1.4 V and the broad asymmetric peak at +0.9 V are assigned to the onset of orbital-mediated tunneling out of the highest occupied molecular orbitals (HOMOs) and into the lowest unoccupied molecular orbitals (LUMOs), respectively.[15,16] Hence, the high-resolution STM images at −1.3 V (Figure 2d) and +0.9 V (Figure 2b) can be interpreted as being dominated by contributions mainly from the HOMO and LUMO, respectively. For investigating the real-space properties of the AuTPP frontier MOs, we additionally performed d*I*/d*V* mapping experiments.[1,2] In d*I*/d*V* mapping, the molecule is scanned in the constant-current mode at a predefined bias voltage while recording the tunneling conductivity, which corresponds to the local density of states (DOS). The bias voltages were chosen to match the HOMO and LUMO energies as determined from the tunneling spectrum. Figure 2e,f shows d*I*/d*V* maps recorded at +0.9 and −1.4 V, designated as the "LUMO map" and "HOMO map", respectively. The HOMO map (Figure 2f) shows the strongest intensity over two opposing pyrrole units, forming a dumbbell-like shape, together with four contributions from the phenyl substituents. The LUMO map (Figure 2e) shows two nodal planes through the center, with the largest conductivity found

10.1021/ja908157j

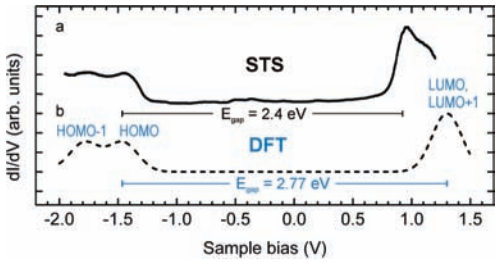

Figure 3. (a) Experimental scanning tunneling spectrum recorded at the center of AuTPP. (b) DFT-calculated best-fit DOS spectrum assuming a saddle conformation and $\Phi = 45°$. The calculated HOMO is matched with the corresponding experimental HOMO energy.

Figure 4. Calculated frontier MOs assuming a saddle geometry of the porphyrin with $\Phi = 45°$ in the gas phase.

over the meso carbon atoms. The similarity of the d*I*/d*V* maps and the STM images in Figure 2b,d is worthy of note.

In contrast to the macrocycle, the position of the metal ion in the center of the molecule appears independent of bias as a depression over the entire voltage range from −1.5 to +1.3 V. The STM signal in the center has been reported to be strongly dependent on the identity of the metal ion.[17] Accordingly, the center has been imaged as a depression for metal ions with doubly occupied atomic valence d states (e.g., Fe^{2+}, Ni^{2+}) and as a protrusion in the case of half-filled ones (e.g., Co^{2+}).[15−18] Thus, the observed dark center in our STM images may provide a hint concerning the oxidation state of the gold ion, as Au^{3+} and Au^{+} have filled d states and Au^{2+} half-filled ones.

To further elucidate the tunneling spectrum, we performed DFT calculations (B3LYP level, LANL2DZ basis set)[19] for AuTPP in the gas phase restricted to saddle conformations with different dihedral angles Φ. Figure 3b shows the calculated DOS spectrum that agreed best with the STS experiment. For the highest occupied MOs, the calculations yield two states, HOMO and HOMO-1, with an energy separation of 0.30 eV. The lowest two unoccupied MOs, LUMO and LUMO+1, are degenerate. A comparison with the tunneling spectrum indeed reveals additional structure in the HOMO and LUMO regions. The HOMO appears as a double peak with an energy splitting of ∼0.35 eV, and the LUMO has a shoulder at higher energies, thus pointing to a double peak. We remark that the calculated best-fit spectrum corresponds to $\Phi = 45°$. Larger Φ values do not reproduce the double-peak configuration for HOMO and HOMO-1, and smaller Φ values overestimate the peak splitting. The calculated energy gap is 2.77 eV, which is comparable to the experimental value of 2.4 eV and nearly independent of Φ. However, its value is ∼0.4 eV larger, which exceeds the experimental error.

Figure 4 depicts calculated representations of the frontier MOs of AuTPP in the gas phase. The geometric shape of the calculated MOs is in qualitative agreement with the experimental d*I*/d*V* maps in Figure 2e,f. Both HOMO and HOMO-1 exhibit a weak deviation from fourfold toward twofold symmetry. LUMO is clearly twofold-symmetric and identical to the degenerate LUMO+1 except for an azimuthal rotation by 90°. A comparison of the experimental LUMO map (Figure 2e) with LUMO and LUMO+1 suggests that STM measured a convolution of energetically adjacent MOs. This explains the observed fourfold symmetry of the experimental LUMO map with strong intensity over the four meso positions and nodal planes through the centers of the pyrroles. In the case of the experimental HOMO map, however, there exists a quantitative discrepancy with the gas-phase DFT calculations, as the observed pronounced dumbbell-like shape (Figure 2f) is not reproduced.

Our combined LT-STM and DFT study reveals the following points: (i) The calculated gas-phase energies of AuTPP are in reasonable agreement with experiment. The observed energy splitting between HOMO and HOMO-1 and the HOMO/LUMO energy gap are well-reproduced by the calculations. (ii) The central depression imaged by constant-current STM is due to doubly occupied d states and excludes Au^{2+} as central ion. Furthermore, our calculations show that the gap energy is 2.7 eV for Au^{3+} and <1 eV for Au^{+}. This allows us to unambiguously identify the oxidation state of the Au ion in the adsorbed AuTPP as Au^{3+}. (iii) The observed deviation between the experimental and calculated gap energies is significant and points to a substantial molecule/substrate interaction. This interpretation is consistent with the recent experimental and theoretical study of Buchner et al.,[17] who reported a similar reduction of the HOMO/LUMO gap by several tenths of electron volts. (iv) Molecule/substrate interactions, which are not included in the gas-phase DFT calculations, may also be responsible for the deviations between the shapes of the d*I*/d*V* maps and the calculated MOs and affect the contribution of the metal ion to the HOMO and LUMO[16] (ligand-to-metal charge transfer[7]), which relates to the electrochemical activity of the complex.

In conclusion, we have characterized for the first time chemotherapeutically relevant AuTPP by LT-STM and STS on the submolecular scale. Our results reveal significant deviations from gas-phase behavior due to a non-negligible molecule/substrate interaction even on a chemically rather inert gold substrate. In that respect, our study can be regarded as a guidepost for future biochemical applications, where conclusive statements will necessitate DFT calculations that also include the details of the biochemical environment.

Acknowledgment. The authors thank the Austrian Science Fund (FWF) for financial support (Projects P20773 and P18384).

Supporting Information Available: Complete refs 11 and 19. This material is available free of charge via the Internet at http://pubs.acs.org.

References

(1) Repp, J.; Meyer, G.; Stojković, S. M.; Gourdon, A.; Joachim, C. *Phys. Rev. Lett.* **2005**, *94*, 026803.
(2) Soe, W.-H.; Manzano, C.; Sarkar, A. D.; Chandrasekhar, N.; Joachim, C. *Phys. Rev. Lett.* **2009**, *102*, 176102.
(3) Knör, G. *Inorg. Chem. Commun.* **2001**, *4*, 160.
(4) Sun, R. W.-Y.; Che, C.-M. *Coord. Chem. Rev.* **2009**, *253*, 1682.
(5) Haeubl, M.; Reith, L. M.; Gruber, B.; Karner, U.; Müller, N.; Knör, G.; Schoefberger, W. *J. Biol. Inorg. Chem.* **2009**, *14*, 1037.
(6) Kadish, K.; Wenbo, E.; Ou, Z.; Shao, J.; Sintic, P.; Ohkubo, K.; Fukuzumi, S.; Crossley, M. *Chem. Commun.* **2002**, 356.
(7) Eng, M.; Ljungdahl, T.; Andreasson, J.; Martensson, J.; Albinsson, B. *J. Phys. Chem. A* **2005**, *109*, 1776.
(8) Ou, Z.; Kadish, K.; Wenbo, E.; Shao, J.; Sintic, P.; Ohkubo, K.; Fukuzumi, S.; Crossley, M. *Inorg. Chem.* **2004**, *43*, 2078.
(9) Barth, J.; Brune, H.; Ertl, G.; Behm, R. *Phys. Rev. B* **1990**, *42*, 9307.
(10) Yokoyama, T.; Yokoyama, S.; Kamikado, T.; Okuno, Y.; Mashiko, S. *Nature* **2001**, *413*, 619.
(11) Brede, J.; et al. *Nanotechnology* **2009**, *20*, 275602.
(12) Yokoyama, T.; Yokoyama, S.; Kamikado, T.; Mashiko, S. *J. Chem. Phys.* **2001**, *115*, 3814.
(13) Auwärter, W.; Klappenberger, F.; Weber-Bargioni, A.; Schiffrin, A.; Strunskus, T.; Wöll, C.; Pennec, Y.; Riemann, A.; Barth, J. V. *J. Am. Chem. Soc.* **2007**, *129*, 11279.
(14) Weber-Bargioni, A.; Auwärter, W.; Klappenberger, F.; Reichert, J.; Lefrancois, S.; Strunskus, T.; Wöll, C.; Schiffrin, A.; Pennec, Y.; Barth, J. V. *ChemPhysChem* **2008**, *9*, 89.
(15) Scudiero, L.; Barlow, D. E.; Hipps, K. W. *J. Phys. Chem. B* **2000**, *104*, 11899.
(16) Scudiero, L.; Barlow, D. E.; Mazur, U.; Hipps, K. W. *J. Am. Chem. Soc.* **2001**, *123*, 4073.
(17) Buchner, F.; Warnick, K.-G.; Wölfle, T.; Görling, A.; Steinrück, H.-P.; Hieringer, W.; Marbach, H. *J. Phys. Chem. C* **2009**, *113*, 16450.
(18) Lu, X.; Hipps, K. W.; Wang, X. D.; Mazur, U. *J. Am. Chem. Soc.* **1996**, *118*, 7197.
(19) Frisch, M. J.; et al. *Gaussian 03*, revision C.02; Gaussian, Inc.: Wallingford, CT, 2004.

JA908157J